TIN2 functions with TPP1/POT1 to stimulate telomerase processivity

Alexandra M. Pike[a,b*], Margaret A. Strong[a], John Paul T. Ouyang[a,c], Carla J. Connelly[a], Carol W. Greider[a,b,c,#]

[a] Department of Molecular Biology and Genetics, Johns Hopkins University School of Medicine, Baltimore, Maryland, USA

[b] Graduate Program in Cellular and Molecular Medicine, Johns Hopkins University School of Medicine, Baltimore, Maryland, USA

[c] Graduate Program in Biochemistry Cell and Molecular Biology, Johns Hopkins University School of Medicine, Baltimore, Maryland, USA

[#]Address correspondence to Carol W. Greider, cgreider@jhmi.edu

* Present Address: Alexandra M. Pike, MIT Department of Biology, Cambridge, Massachusetts

Running Title

TIN2 stimulates telomerase processivity

Word Count: Text - 4620; Materials and Methods – 1685

Keywords:

Telomerase; telomere; TIN2; telomere syndromes; alternative splicing; shelterin; TPP1; POT1; processivity

Abstract

Telomere length maintenance is crucial for cells that divide many times. TIN2 is an important regulator of telomere length, and mutations in *TINF2*, the gene encoding TIN2, cause short telomere syndromes. While the genetics underscore the importance of TIN2, the mechanism through which TIN2 regulates telomere length remains unclear. Here, we characterize the effects of TIN2 on telomerase activity. We identified a new isoform in human cells, TIN2M, that is expressed at similar levels to previously studied TIN2 isoforms. Additionally, we found that all three TIN2 isoforms stimulated telomerase processivity beyond the previously characterized stimulation by TPP1/POT1. Mutations in the TPP1 TEL-patch abrogated this stimulation, implicating TIN2 as a component of the TPP1/POT1 processivity complex. All three TIN2 isoforms localized to telomeres *in vivo* but had distinct effects on telomere length, suggesting they are functionally distinct. These data contrast previous descriptions of TIN2 a simple scaffolding protein, showing that TIN2 isoforms directly regulate telomerase.

Importance

Telomere length regulation maintains the fine balance between cancer and short telomere syndromes, which are complex degenerative diseases including bone marrow failure and pulmonary fibrosis. The enzyme telomerase maintains telomere equilibrium through highly regulated addition of telomere sequence to chromosome ends. Here, we uncover a previously unknown biochemical role for human shelterin component TIN2 in regulating telomerase enzyme processivity and suggest that TIN2 functions with

45 TPP1/POT1 as a specialized telomeric single-stranded DNA-binding complex.
46 Additionally, CRISPR/Cas9 genome editing revealed a new TIN2 isoform expressed in
47 human cells, and we showed that the three TIN2 isoforms have different effects on
48 telomere length. These findings suggest that previous descriptions of TIN2 as a tethering
49 or bridging protein is incomplete and reveal a previously unappreciated complexity in
50 telomere length regulation. This new perspective on shelterin components regulating
51 telomere length at the molecular level will help advance understanding of clinical
52 manifestations of short telomere syndromes.
53

Introduction

Telomere length in human cells is maintained around a tight equilibrium that prevents life-threatening disease. Telomere shortening leads to a characteristic set of degenerative diseases, including pulmonary fibrosis, bone marrow failure, and immune deficiency, collectively called short telomere syndromes(1). In contrast, 90% of human cancers upregulate telomerase, and mutations that increase telomerase levels predispose to cancer(2–4). While we understand many component pathways that regulate telomere length, a detailed integrated mechanism of telomere length regulation is not fully understood.

Human telomeres consist of about 10kb of TTAGGG repeats, that are mostly double-stranded DNA with a single-stranded 3' overhang, all bound by a protein complex termed shelterin(5). This DNA-protein complex protects chromosome ends, and shelterin both positively and negatively regulates telomere repeat addition by telomerase. The shelterin complex consists of six subunits: two double-stranded DNA binding proteins TRF1 and TRF2(6–9), a single-stranded telomeric binding protein POT1(10, 11), as well as interacting proteins TPP1, TIN2, and RAP1(12–16).

POT1 and TPP1 form a heterodimer that binds single stranded telomeric DNA and stimulates telomerase processivity *in vivo* and *in vitro*(17–19). This stimulation is mediated though the TPP1 OB-fold, which contains conserved TEL-patch and NOB regions that directly interact with the TEN domain of TERT(20–23). Mutations in the TEL-patch abrogate the stimulation of processivity, and compensatory charge swap

mutations in TERT restore function(24), suggesting the direct binding of TPP1/POT1 heterodimer to TERT mediates processivity.

TIN2, encoded by the *TINF2* gene, localizes to telomeres through interactions with TRF1, TRF2, and TPP1 (Figure 1A, B). TIN2 interaction with TPP1 is essential for TPP1/POT1 localization and function in cells(25–28). TIN2 also binds to the double stranded DNA binding proteins TRF1 and TRF2(12, 29). Knocking down TIN2 also causes loss of TRF1 and TRF2 at telomeres, suggesting that TIN2 stabilizes TRF1 and TRF2 binding to telomeres(29). Because of its interactions with TRF1, TRF2, and TPP1/POT1, TIN2 has been described as a molecular bridge between the dsDNA- and ssDNA-binding shelterin components. However, it is likely that TIN2 performs additional telomeric functions, as shelterin may consist of distinct functional subcomplexes as implied by genetic and biochemical experiments(29–33).

TINF2 mutations cause autosomal dominant inheritance of short telomere syndromes, including dyskeratosis congenita(34, 35) and pulmonary fibrosis(36–38). These mutations are often *de novo*, causing severe disease in patients heterozygous for the mutant allele. These germline missense or nonsense mutations in TIN2 are clustered in a small domain of unknown function (Figure 1B)(34, 35, 39). Within this domain, K280 and R282 are the most commonly mutated residues, and K280E, K280X, R282S, and R282H are the most widely studied TIN2 mutations. These mutant proteins are expressed and stable. In addition to TIN2, mutations in TPP1 and POT1 also cause short telomere disease. The TPP1-ΔK170 mutation deforms the TEN domain binding interface and disrupts the TPP1-telomerase interaction, leading to decreased telomerase

processivity(40–42). A POT1-S322L mutation in Coats plus is thought to cause short telomeres through defective telomere replication(43). While mutations in many different genes cause telomere shortening in patients(3), TIN2, TPP1, and POT1 are the only shelterin proteins with mutations identified in short telomere syndromes to date.

Several mechanisms have been proposed for telomere shortening caused by *TINF2* mutations, including defects in telomerase recruitment(44) or decreased telomerase association with the telomere(45). Others have argued for telomerase-independent mechanisms of telomere shortening(46, 47). Several lines of evidence suggest that the TIN2 patient mutations function in a dominant negative manner(34, 37, 45), however, the molecular nature of this effect is not yet understood. To elucidate the mechanism of telomere shortening, we set out to test the biochemical functions of the TIN2 isoforms. We identified a new isoform, TIN2M, and found that all three TIN2 isoforms stimulate telomerase processivity in a TPP1/POT1 dependent manner. The three isoforms had different effects on telomere length when overexpressed in human cells, suggesting functional differences *in vivo.*

Results

Identification of a new TIN2 isoform, TIN2M

Human TIN2 is alternatively spliced into two previously described isoforms, TIN2S and TIN2L(12, 48). Most prior work has been performed using the shorter human TIN2S, which was described first, or in the mouse TIN2, which only has one isoform.

TIN2L encompasses all 354 amino acids of TIN2S with an additional 97 C-terminal amino acid residues(48), including a highly conserved domain (Figure 1B)(49). To study TIN2 function *in vivo*, we knocked in an N-terminal myc epitope tag at the endogenous *TINF2* locus in 293T cells using CRISPR/Cas9 genome editing (Supplementary Figure 1A).

Western blots on several edited clones unexpectedly showed three distinct bands, instead of the expected two bands of the known isoforms (Supplementary Figure 1B). To further examine these isoforms, we cloned a myc-tagged full-length *TINF2* gene, including all introns, into an expression vector with the CMV promoter. In transfected cells overexpressing this construct alongside TIN2S or TIN2L cDNA, we again observed an intermediate sized band at approximately 47 kDa. (Figure 1C).

To test whether this band corresponds to an alternatively spliced TIN2 isoform, we used a modified 3' RACE with PacBio sequencing to identify all full-length expressed isoforms in human and mouse cells. In 293T cells, TIN2S and TIN2L cDNAs were identified along with a third major isoform, which would encode the expected molecular weight for the unknown protein. We termed this isoform TIN2M for TIN2 "medium". TIN2M results from retention of the last intron, between exons 8 and 9, that encodes 13 amino acids of unique sequence ($_{408}$-VSGKEQKAGKGDG-$_{420}$) before reaching a stop codon (Figure 1D-E). Sequence read counts indicated that TIN2M and TIN2L mRNAs were expressed at similar levels, while TIN2S had 2-fold greater representation than each of the others, suggesting it is the predominant transcript (Figure 1D and Supplementary Figure 2A). 3' RACE further showed that TIN2M was present at

similar levels in four other human cell lines (HeLa, K562, RPE-1, and a newly derived LCL) (Figure 1E). In addition to these three major isoforms in human cells, we identified a number of additional recurrent exon skipping, intron retention, and alternative polyadenylation site usage events, including exon 2 skipping described previously(50) (Supplementary Figure 2A). We found that two different mouse strains (C57BL/6 and CAST/EiJ) expressed just one TIN2 isoform that is most similar to TIN2L, as previously described(48, 51) (Supplementary Figure 2B).

Evidence for expression of TIN2M was also found in publicly available data from PacBio IsoSeq of MCF-7 breast cancer cells (http://www.pacb.com/blog/data-release-human-mcf-7-transcriptome/). Additionally, genome-wide ribosome profiling data from GWIPS-viz shows ribosome peaks present in the unique coding region of the TIN2M retained intron(52). TIN2M and TIN2L, but not TIN2S, contain the recently identified CK2 phosphorylation site(49). All three of the expressed isoforms contain the documented cluster of telomere syndrome patient mutations and the other known interaction domains, suggesting that any of these three isoforms could mediate the short telomere phenotypes seen *in vivo*.

TIN2 cooperates with TPP1/POT1 to stimulate telomerase processivity

TIN2 interacts directly with TPP1, a processivity factor that heterodimerizes with POT1 and directly binds telomerase through the TPP1 TEL-patch domain(18, 20–22, 53). To examine whether TIN2 affects telomerase activity or processivity, we adapted the

cell-based system overexpressing TERT, TR, POT1, and TPP1 used by Nandakumar *et al* (20). By co-overexpressing TERT, TR, TPP1, and POT1 in cells, cell lysates can be used in direct telomerase activity assays(18–20, 54). Because endogenous telomere proteins are expressed at low levels, the telomerase activity observed in this system result from the overexpressed proteins. We adapted this system to generate cells constitutively expressing TERT, TR, TPP1, and POT1, where TIN2 can be introduced by transient transfection.

For reproducible overexpression of the protein components, we created a polycistronic expression cassette containing FLAG-TPP1, FLAG-POT1, and FLAG-TERT separated by 2A peptides (Figure 2A and Supplementary Figure 3A). As a negative control, we mutated the TPP1 TEL-patch (TPP1 E169A/E171A)(20), referred to here as $TPP1^{TEL}$, to test whether any effects of TIN2 are mediated through TPP1/POT1 stimulation of telomerase (Figure 2A and Supplementary Figure 3B). Then, we generated a clonal cell line overexpressing TR in 293TREx FLP-in cells, into which we integrated the respective expression cassette at a unique genomic locus using the FLP-in system. The resulting cell lines are referred to as TPP1/POT1/TERT and $TPP1^{TEL}$/POT1/TERT (Figure 2A-C).

To examine the interaction of TIN2 with TPP1/POT1 and telomerase, the three TIN2 isoforms were individually transfected into each cell line. Each of the three TIN2 isoforms reproducibly co-immunoprecipitated with TPP1/POT1 and TERT in reciprocal pull downs of either myc-TIN2 or FLAG-TPP1/POT1/TERT (Figure 2D and Supplementary Figure 4). We observed no change in co-immunoprecipitation of

TPP1/POT1 and TERT with TIN2 when any of the three isoforms carried one of the common patient mutations, K280E (Figure 2D), as previously reported for the TIN2S isoform(44, 55). Telomerase activity can be detected in these co-immunoprecipitations, suggesting that the telomerase in complex with TIN2 is active (data not shown). We conclude that all three isoforms of TIN2 are interacting with TPP1/POT1 in complex with active telomerase, and the K280E patient mutation does not disrupt this interaction.

To examine the effects of TIN2 on telomerase activity, we transfected the myc-tagged full length gene, myc-*TINF2*, into the TPP1/POT1/TERT cell line. All three isoforms were expressed from the myc-*TINF2* construct and the lysates showed an increase in processivity compared to the GFP control (Supplementary Figure 5), suggesting that TIN2 enhances telomerase processivity over the effects of TPP1/POT1 alone. To determine if specific TIN2 isoforms are required for this stimulation, we independently transfected each isoform into the TPP1/POT1/TERT cell line (Figure 3A). We found a reproducible 10-20% stimulation of telomerase processivity with each of the three N-terminally tagged isoforms (Figure 3B-C). To test whether TIN2 stimulation of telomerase depends on TPP1/POT1, we transfected TIN2 into $TPP1^{TEL}$/POT1/TERT cells and separately into a TERT-only cell line overexpressing TERT/TR but not TPP1/POT1. We found no stimulation of telomerase processivity in either of these cell lines (Figure 3A-C and Supplementary Figure 6), suggesting the stimulation is dependent on TPP1/POT1. Our results indicate that TIN2 cooperates with TPP1/POT1 to stimulate telomerase processivity.

Because all three TIN2 isoforms stimulated telomerase to the same extent in a TPP1/POT1 dependent manner, we tested whether patient mutations TIN2-K280E, TIN2-R282S, TIN2-R282H, or TIN2-K280X affect processivity. In some instances, we found that TIN2 mutants were deficient at stimulating telomerase activity, but this result was variable both in whole-cell lysates and in TIN2 co-immunoprecipitations (Supplementary Figure 5 and data not shown). Because the mutants are dominant-negative *in vivo*, we tried co-expressing wild-type TIN2 with a mutant TIN2, but there was no change in processivity stimulation in this setting (Supplementary Figure 7). Although the patient mutations did not reproducibly affect telomerase processivity, we have identified a previously unknown role of TIN2 isoforms in telomerase processivity stimulation that changes the understanding of TIN2's role in telomere length regulation.

TIN2 isoforms localize to telomeres and have different effects on telomere length

Since all TIN2 isoforms stimulated telomerase in a TPP1/POT1 dependent manner, we examined whether they function differently in human cells. TIN2S and TIN2L have been demonstrated to localize to telomeres *in vivo* through interaction with TRF1 and TRF2(12, 48). Patient mutations did not disrupt the localization of TIN2S(44), but localization of TIN2L with patient mutations has not been reported. To determine whether TIN2M localizes to telomeres and whether patient mutations affect localization of TIN2M or TIN2L, we examined the localization of each isoform with or without the K280E patient mutation.

Because of the alternative splicing of *TINF2* transcripts, we could not test expression of individual isoforms at the endogenous locus. Instead, we stably overexpressed cDNA encoding TIN2S, TIN2M, or TIN2L with or without the K280E patient mutation in HeLa-FRT Flp-in cells (Figure 4A). Using this system, the expression constructs were integrated at a unique genomic locus, and isogenic, polyclonal cell lines were selected. Western blot analysis showed similar expression levels of TIN2S, TIN2M, and TIN2L that was not affected by the K280E mutation (Figure 4A). Using indirect immunofluorescence, we found that all three isoforms, with or without the K280E patient mutation, showed discrete foci that co-localized with TRF2, indicating that they each localize to telomeres *in vivo* (Figure 4B).

Previous work has shown that overexpression of wild-type TIN2S had little effect on telomere length, while overexpression of TIN2S-K280E, TIN2S-R282S, or TIN2S-R282H decreased telomere length(12, 44). A recent study showed overexpression of TIN2L resulted in some increase in telomere length(49). Having these isoform-specific polyclonal TIN2 overexpressing cell lines in hand, we examined how the TIN2 constructs affect telomere length. We passaged these cells and monitored telomere length by Southern blot and q-FISH analysis. TIN2S, TIN2S-K280E, and the control GFP cell lines showed no significant changes in telomere length over time (Figure 4C-D). In contrast, TIN2L showed some telomere elongation, and TIN2M, TIN2M-K280E, and TIN2L-K280E showed significant increases in telomere length (Figure 4C-D). The excessive telomere elongation resembles the telomere elongation in a number of TPP1/POT1 loss of function mutants(12, 13, 31, 44, 56). These telomere length changes are not due to

clonal variation, as our cells are a mixed clonal population of isogenic cells. Telomere length effects appear to differ between immortalized cell lines, as TIN2 overexpression had little effect on telomere length in 293TREx cells (data not shown). The observation that the different TIN2 isoforms and mutants do have strong yet different effects in HeLa cells suggests that these isoforms play different functional roles in the cell.

We next examined telomere aberrations in blinded q-FISH images. We saw no changes in signal-free ends, PQ ratios, sister telomere heterogeneity, or telomere fusions (Supplementary Figure 8). However, we found a variable but elevated incidence of telomere doublets, or fragile telomeres, which are indicative of telomere replication defects, in cells overexpressing TIN2M and the mutant isoforms TIN2S-K280E, TIN2M-K280E, and TIN2L-K280E (Supplementary Figure 8A). These results support the conclusion that the telomere elongation is due to an effect of TIN2 on TPP1/POT1 function and further suggest that TIN2 participates with TPP1 and POT1 in facilitating telomere replication as well as stimulating telomerase processivity.

Discussion

We have identified a new isoform of TIN2, TIN2M, and have shown that each of the three TIN2 isoforms cooperate with TPP1/POT1 to stimulate telomerase processivity. We found that the TIN2 isoforms play different roles in telomere length regulation in cells. Our data suggest that TIN2 forms a functional shelterin subcomplex with TPP1/POT1. Considering TIN2 as part of the telomerase processivity complex provides a new way to think about its role in telomere length regulation.

The mutations in *TINF2* in short telomere syndrome patients mostly cluster in a TIN2 domain of unknown function in exon 6 near the C-terminus of TIN2(34, 35). Genetic evidence strongly supports a dominant negative mechanism for the mutant TIN2 proteins. First, TIN2 mutations have autosomal dominant inheritance. The mutant proteins are stably expressed and cause telomere shortening despite the presence of a wild-type TIN2. Secondly, the clustering of disease associated alleles rather than distribution across the coding sequence suggests these are not simply inactivating mutations but rather a gain of function. Finally, there is evidence for selection against the mutant proteins in the hematopoietic lineage *in vivo*(37). The dominant negative mechanism is also supported by experimental evidence(45), but the molecular nature of this effect is not well understood.

TIN2 C-terminus plays an essential role in telomere length regulation

We found that all three TIN2 isoforms form a complex with TPP1/POT1, stimulate telomerase processivity, and localize to telomeres, yet have different effects on telomere length in cells, underscoring the important role of the TIN2 C-terminus. TIN2 can be divided into two regions: the shelterin-interacting region in the N-terminus, and the C-terminal region that includes the patient mutation cluster, the variable C-terminal extensions of TIN2M and TIN2L, and several other interaction sites and modifications(47, 49, 57, 58) (Figure 1B). All three isoforms contain the shelterin-interacting domain and patient mutation cluster, varying only in the C-terminal extension after E354.

The structure is known for much of the shelterin-interacting region, including the N-terminal TRF2/TPP1 binding domain ($TIN2_{1-202}$)(59) and the short TRF1-interacting motif ($TIN2_{256-276}$)(60). There is no structural information, however, for the C-terminal region, including both the mutation hotspot and the variable C-terminal extension, which contains a highly conserved region with a CK2 phosphorylation site at S396(49). Interestingly, some of the patient mutations are truncations, such as K280X, that generate a short stable protein missing the entire C-terminal region(39). Previous work indicated the importance of the TIN2 C-terminal region, including the high degree of conservation the variable C-terminal extension and the dominant effects of C-terminal truncating mutations. Our work further supports this idea, with discovery of a TIN2 isoform with an alternative C-terminal region and evidence that overexpression of only the isoforms containing C-terminal extensions strongly affect telomere length (Figure 4C,D and (49)). The TIN2 C-terminus may function through binding a novel partner, or through a conformational or structural role.

TIN2 cooperates with TPP1/POT1 to stimulate telomerase processivity

Our studies indicate that TIN2 is part of the telomerase processivity factor (Figure 5A). All three TIN2 isoforms formed a stable complex with TPP1/POT1 and TERT and further stimulated telomerase processivity over that of TPP1/POT1 alone. This stimulation of processivity required TPP1 and POT1, as there was no stimulation in cells expressing TPP1 TEL-patch mutants or TERT alone (Figure 3 and Supplementary Figure 6). TIN2 could enhance telomerase processivity by improving the TPP1/POT1 complex

stability or its interaction with telomerase, or by promoting the telomeric ssDNA interaction of the complex, or some combination of these (Figure 5A).

Interestingly, the identification of TIN2 as an additional component to an already known processivity factor is reminiscent of recent findings in *Tetrahymena*. The *Tetrahymena* telomerase holoenzyme structure(61) revealed previously unknown subunits, Teb2 and Teb3, that interact with the previously defined Teb1-p50 processivity complex. The addition of these proteins to *in vitro* reactions further stimulated telomerase processivity, possibly by stabilizing the complete, assembled, processive enzyme complex(62). Further, this structure revealed that the telomerase holoenzyme contains two single-stranded DNA binding complexes: the p50/TEB processivity factor, which stimulates telomeric G-strand synthesis by telomerase, and the CST complex, which stimulates telomeric C-strand synthesis by lagging strand replication machinery. This is the first evidence of physical coupling of two telomere maintenance processes that have long been known to be coupled *in vivo* (reviewed in(63)).

Our results with TIN2 parallel the discovery of the missing components of the TEB processivity complex in *Tetrahymena*(61, 62), suggesting that TIN2 binding to TPP1/POT1 stabilizes the complex and thus promotes processivity. Interestingly, CST (CTC1/STN1/TEN1), a second ssDNA telomeric complex, interacts with TPP1/POT1 to limit telomere extension by coupling C-strand to G-strand synthesis(64, 65). The C-terminal region of TIN2 is a candidate for coupling TIN2/TPP1/POT1 with CST for coordinated C- and G-strand synthesis, affecting both positive and negative telomere length regulation. Decreased telomerase activity leads to gradual telomere shortening

over many generations. Partial uncoupling of telomerase elongation from C-strand synthesis, however, could cause unrestrained telomerase elongation of telomeres, while complete uncoupling could result in telomere shortening by failure to synthesize either C- or G-strands.

TIN2/TPP1/POT1 is a telomere specific single-stranded binding complex involved in telomere extension and replication

Our data, in combination with previously published work, suggest that TIN2/TPP1/POT1 is a shelterin subcomplex. TIN2 not only increases the processivity stimulation of the complex but also promotes its telomeric localization *in vivo* (Figure 5A). Evidence from previous work supports this conclusion. First, when TRF1 is removed from telomeres by tankyrase-1 modification, TIN2/TPP1 remain at telomeres (13). Second, posttranslational depletion of TIN2 by Siah2 ubiquitination removes TPP1 but not TRF1 or TRF2 from telomeres(57). Further evidence in TIN2 floxed mouse cell lines or TIN2 knockdown in HeLa cells show reduced telomeric TPP1/POT1 localization(26, 27). Similarly, disruption of the TIN2 TRF1-binding motif does not disrupt TRF1, TRF2, or Rap1 localization, but prevents TIN2/TPP1/POT1 accumulation at telomeres in mouse cells(25). Deletion of the TPP1-binding region from mouse TIN2 also prevents localization of TPP1/POT1 to telomeres(28). Finally, genetic evidence using CRISPR knockouts in human cells led the authors to conclude that TIN2/TPP1/POT1 is a shelterin subcomplex(30). These findings together with our work showing the stimulation of

telomerase processivity, further supports the conclusion that TIN2, TPP1, and POT1 function together as a subcomplex of shelterin.

The TIN2/TPP1/POT1 heterotrimer likely affects both telomerase and replication fork progression. Considering TIN2/TPP1/POT1 as a telomere specific ssDNA binding (SSB) protein complex helps explain defects in telomere replication that have been reported for both POT1 and TPP1 knockdowns and mutants(12, 13, 31, 44, 56). While most diagrams draw TPP1/POT1 bound to the G-strand overhang at telomeres, this telomere specific SSB complex can also bind the telomeric G-strand exposed during DNA replication(26, 66) (Figure 5B).

TPP1 and POT1 have both been reported to facilitate DNA replication through telomeric tracts(64, 67–69). POT1 mutants that cannot bind DNA cause telomere replication fork stalling, fragile telomeres, and ATR activation(69), possibly due to ssDNA exposure at the telomeric replication fork. TIN2 knockdown(26) and mouse mutants(46) also cause an ATR-mediated DNA damage response. We found that overexpression of some of the TIN2 isoforms resulted in fragile telomeres indicative of telomere replication defects (Figure S8). Taken together, this suggests that the telomeric TIN2/TPP1/POT1and CST complexes may participate directly in replication fork progression through the telomere, and that perturbation of this function may lead to replication fork collapse and activation of ATR.

The interpretation of TIN2/TPP1/POT1 as a ssDNA binding shelterin subcomplex provides an updated view of TIN2's role in telomere length regulation. We found that TIN2 is expressed as multiple isoforms that have different effects on telomere length in

373 human cells. Strikingly, we found that TIN2 is a previously unappreciated component of
374 the telomerase processivity complex. All three isoforms stimulated telomerase
375 processivity in a TPP1/POT1 dependent manner. Further biochemical work on this
376 heterotrimeric ssDNA telomere binding protein will elucidate the mechanism of TIN2
377 regulation of telomere length and how it is disrupted in short telomere syndromes.

378 ## References

379 1. Armanios M, Blackburn EH. 2012. The telomere syndromes. Nat Rev Genet
380 13:693–704.
381 2. Kim NW, Piatyszek MA, Prowse KR, Harley CB, West D, Ho PLC, Coviello GM,
382 Wright WE, Weinrich SL, Shay W, West MD, Shay JW. 1994. Specific
383 Association of Human Telomerase Activity with Immortal Cells and Cancer.
384 Science (80-) 266:2011–2015.
385 3. Stanley SE, Armanios M. 2015. The short and long telomere syndromes: Paired
386 paradigms for molecular medicine. Curr Opin Genet Dev 33:1–9.
387 4. Horn S, Figl A, Rachakonda PS, Fischer C, Sucker A, Gast A, Kadel S, Moll I,
388 Nagore E, Hemminki K, Schadendorf D, Kumar R. 2013. TERT promoter
389 mutations in familial and sporadic melanoma. Science 339:959–61.
390 5. Palm W, de Lange T. 2008. How Shelterin Protects Mammalian Telomeres. Annu
391 Rev Genet 42:301–334.
392 6. Zhong Z, Shiue L, Kaplan S, de Lange T. 1992. A mammalian factor that binds
393 telomeric TTAGGG repeats in vitro. Mol Cell Biol 12:4834–4843.

7. Bilaud T, Brun C, Ancelin K, Koering CE, Laroche T, Gilson E. 1997. Telomeric localization of TRF2, a novel human telobox protein. Nat Genet 17:236–9.

8. Bianchi A, Smith S, Chong L, Elias P, de Lange T. 1997. TRF1 is a dimer and bends telomeric DNA. EMBO J 16:1785–1794.

9. Broccoli D, Smogorzewska A, Chong L, de Lange T. 1997. Human telomeres contain two distinct Myb-related proteins, TRF1 and TRF2. Nat Genet 17:231–235.

10. Baumann P, Cech TR. 2001. Pot1, the Putative Telomere End-Binding Protein in Fission Yeast and Humans. Science (80-) 292:1171–1175.

11. Baumann P, Podell E, Cech TR. 2002. Human Pot1 (protection of telomeres) protein: cytolocalization, gene structure, and alternative splicing. Mol Cell Biol 22:8079–87.

12. Kim SH, Kaminker P, Campisi J. 1999. TIN2, a new regulator of telomere length in human cells. Nat Genet 23:405–412.

13. Houghtaling BR, Cuttonaro L, Chang W, Smith S. 2004. A dynamic molecular link between the telomere length regulator TRF1 and the chromosome end protector TRF2. Curr Biol 14:1621–1631.

14. Ye JZ, Hockemeyer D, Krutchinsky AN, Loayza D, Hooper SM, Chait BT, de Lange T. 2004. POT1-interacting protein PIP1: a telomere length regulator that recruits POT1 to the TIN2/TRF1 complex. Genes Dev 18:1649–1654.

15. Liu D, Safari A, O'Connor MS, Chan DW, Laegeler A, Qin J, Songyang Z. 2004. PTOP interacts with POT1 and regulates its localization to telomeres. Nat Cell

Biol 6:673–680.

16. Li B, Oestreich S, de Lange T. 2000. Identification of human Rap1: implications for telomere evolution. Cell 101:471–483.

17. Lei M, Zaug AJ, Podell ER, Cech TR. 2005. Switching human telomerase on and off with hPOT1 protein in vitro. J Biol Chem 280:20449–20456.

18. Wang F, Podell ER, Zaug AJ, Yang Y, Baciu P, Cech TR, Lei M. 2007. The POT1-TPP1 telomere complex is a telomerase processivity factor. Nature 445:506–10.

19. Latrick CM, Cech TR. 2010. POT1-TPP1 enhances telomerase processivity by slowing primer dissociation and aiding translocation. EMBO J 29:924–33.

20. Nandakumar J, Bell CF, Weidenfeld I, Zaug AJ, Leinwand LA, Cech TR. 2012. The TEL patch of telomere protein TPP1 mediates telomerase recruitment and processivity. Nature 492:285–289.

21. Sexton AN, Youmans DT, Collins K. 2012. Specificity requirements for human telomere protein interaction with telomerase holoenzyme. J Biol Chem 287:34455–34464.

22. Zhong FL, Batista LFZ, Freund A, Pech MF, Venteicher AS, Artandi SE. 2012. TPP1 OB-fold domain controls telomere maintenance by recruiting telomerase to chromosome ends. Cell 150:481–494.

23. Grill S, Tesmer VM, Nandakumar J. 2018. The N Terminus of the OB Domain of Telomere Protein TPP1 Is Critical for Telomerase Action. Cell Rep 22:1132–1140.

24. Schmidt JC, Dalby AB, Cech TR. 2014. Identification of human TERT elements

438 necessary for telomerase recruitment to telomeres. Elife 3:1–20.

439 25. Frescas D, de Lange T. 2014. TRF2-tethered TIN2 can mediate telomere
440 protection by TPP1/POT1. Mol Cell Biol 34:1349–1362.

441 26. Takai KK, Kibe T, Donigian JR, Frescas D, de Lange T. 2011. Telomere
442 protection by TPP1/POT1 requires tethering to TIN2. Mol Cell 44:647–659.

443 27. Abreu E, Aritonovska E, Reichenbach P, Cristofari G, Culp B, Terns RM, Lingner
444 J, Terns MP. 2010. TIN2-tethered TPP1 recruits human telomerase to telomeres in
445 vivo. Mol Cell Biol 30:2971–2982.

446 28. Frescas D, De Lange T. 2014. Binding of TPP1 protein to TIN2 protein is required
447 for POT1a,b protein-mediated telomere protection. J Biol Chem 289:24180–
448 24187.

449 29. Ye JZ, Donigian JR, van Overbeek M, Loayza D, Luo Y, Krutchinsky AN, Chait
450 BT, de Lange T. 2004. TIN2 binds TRF1 and TRF2 simultaneously and stabilizes
451 the TRF2 complex on telomeres. J Biol Chem 279:47264–47271.

452 30. Kim H, Li F, He Q, Deng T, Xu J, Jin F, Coarfa C, Putluri N, Liu D, Songyang Z.
453 2017. Systematic analysis of human telomeric dysfunction using inducible
454 telosome/shelterin CRISPR/Cas9 knockout cells. Cell Discov 3:17034.

455 31. O'Connor MS, Safari A, Xin H, Liu D, Songyang Z. 2006. A critical role for TPP1
456 and TIN2 interaction in high-order telomeric complex assembly. Proc Natl Acad
457 Sci U S A 103:11874–11879.

458 32. Liu D, O'Connor MS, Qin J, Songyang Z. 2004. Telosome, a mammalian
459 telomere-associated complex formed by multiple telomeric proteins. J Biol Chem

279:51338–51342.

33. Lim CJ, Zaug AJ, Kim HJ, Cech TR. 2017. Reconstitution of human shelterin complexes reveals unexpected stoichiometry and dual pathways to enhance telomerase processivity. Nat Commun 8:1075.

34. Savage SA, Giri N, Baerlocher GM, Orr N, Lansdorp PM, Alter BP. 2008. TINF2, a component of the shelterin telomere protection complex, is mutated in dyskeratosis congenita. Am J Hum Genet 82:501–509.

35. Walne AJ, Vulliamy T, Beswick R, Kirwan M, Dokal I. 2008. TINF2 mutations result in very short telomeres: analysis of a large cohort of patients with dyskeratosis congenita and related bone marrow failure syndromes. Blood 112:3594–3600.

36. Fukuhara A, Tanino Y, Ishii T, Inokoshi Y, Saito K, Fukuhara N, Sato S, Saito J, Ishida T, Yamaguchi H, Munakata M. 2013. Pulmonary fibrosis in dyskeratosis congenita with TINF2 gene mutation. Eur Respir J 42:1757–9.

37. Alder JK, Stanley SE, Wagner CL, Hamilton M, Hanumanthu VS, Armanios M. 2015. Exome sequencing identifies mutant TINF2 in a family with pulmonary fibrosis. Chest 147:1361–1368.

38. Hoffman TW, van der Vis JJ, van Oosterhout MFM, van Es HW, van Kessel DA, Grutters JC, van Moorsel CHM. 2016. TINF2 Gene Mutation in a Patient with Pulmonary Fibrosis. Case Rep Pulmonol 2016:1310862.

39. Sasa GS, Ribes-Zamora A, Nelson ND, Bertuch AA. 2012. Three novel truncating TINF2 mutations causing severe dyskeratosis congenita in early childhood. Clin

Genet 81:470–478.

40. Guo Y, Kartawinata M, Li J, Pickett HA, Teo J, Kilo T, Barbaro PM, Keating B, Chen Y, Tian L, Al-Odaib A, Reddel RR, Christodoulou J, Xu X, Hakonarson H, Bryan TM. 2014. Inherited bone marrow failure associated with germline mutation of ACD, the gene encoding telomere protein TPP1. Blood 124:2767–74.

41. Kocak H, Ballew BJ, Bisht K, Eggebeen R, Hicks BD, Suman S, O'Neil A, Giri N, Maillard I, Alter BP, Keegan CE, Nandakumar J, Savage SA, Bass S, Boland J, Burdett L, Chowdhury S, Cullen M, Dagnall C, Higson H, Hutchinson AA, Jones K, Larson S, Lashley K, Lee HJ, Luo W, Malasky M, Manning M, Mitchell J, Roberson D, Vogt A, Wang M, Yeager M, Zhang X, Caporaso NE, Chanock SJ, Greene MH, Goldin LR, Goldstein AM, Hildesheim A, Hu N, Landi MT, Loud J, Mai PL, McMaster ML, Mirabello L, Morton L, Parry D, Pathak A, Rotunno M, Stewart DR, Taylor P, Tobias GS, Tucker MA, Wong J, Yang XR, Yu G, Maillard I, Alter BP, Keegan CE, Nandakumar J, Savage SA. 2014. Hoyeraal-Hreidarsson syndrome caused by a germline mutation in the TEL patch of the telomere protein TPP1. Genes Dev 28:2090–102.

42. Bisht K, Smith EM, Tesmer VM, Nandakumar J. 2016. Structural and functional consequences of a disease mutation in the telomere protein TPP1. Proc Natl Acad Sci U S A 201605685.

43. Takai H, Jenkinson E, Kabir S, Babul-Hirji R, Najm-Tehrani N, Chitayat DA, Crow YJ, de Lange T. 2016. A POT1 mutation implicates defective telomere end fill-in and telomere truncations in Coats plus. Genes Dev 30:812–826.

504 44. Yang D, He Q, Kim H, Ma W, Songyang Z. 2011. TIN2 protein dyskeratosis
505 congenita missense mutants are defective in association with telomerase. J Biol
506 Chem 286:23022–23030.
507 45. Frank AK, Tran DC, Qu RW, Stohr BA, Segal DJ, Xu L. 2015. The Shelterin
508 TIN2 Subunit Mediates Recruitment of Telomerase to Telomeres. PLoS Genet
509 11:1–19.
510 46. Frescas D, de Lange T. 2014. A TIN2 dyskeratosis congenita mutation causes
511 telomerase-independent telomere shortening in mice. Genes Dev 28:153–166.
512 47. Canudas S, Houghtaling BR, Bhanot M, Sasa G, Savage SA, Bertuch AA, Smith
513 S. 2011. A role for heterochromatin protein 1gamma at human telomeres. Genes
514 Dev 25:1807–1819.
515 48. Kaminker PG, Kim SH, Desprez PY, Campisi J. 2009. A novel form of the
516 telomere-associated protein TIN2 localizes to the nuclear matrix. Cell Cycle
517 8:931–939.
518 49. Nelson ND, Dodson LM, Escudero L, Sukumar AT, Williams CL, Mihalek I,
519 Baldan A, Baird DM, Bertuch AA. 2018. The C-terminal extension unique to the
520 long isoform of the shelterin component TIN2 enhances its interaction with TRF2
521 in a phosphorylation- and dyskeratosis congenita-cluster-dependent fashion. Mol
522 Cell Biol MCB.00025-18.
523 50. Ishdorj G, Kost SEF, Beiggi S, Zang Y, Gibson SB, Johnston JB. 2017. A novel
524 spliced variant of the TIN2 shelterin is present in chronic lymphocytic leukemia.
525 Leuk Res 59:66–74.

526 51. Kim SH, Parrinello S, Kim J, Campisi J. 2003. Mus musculus and Mus spretus
527 homologues of the human telomere-associated protein TIN2. Genomics 81:422–
528 432.
529 52. Michel AM, Fox G, M. Kiran A, De Bo C, O'Connor PBF, Heaphy SM, Mullan
530 JPA, Donohue CA, Higgins DG, Baranov P V. 2014. GWIPS-viz: Development of
531 a ribo-seq genome browser. Nucleic Acids Res 42:D859–D864.
532 53. Zaug AJ, Podell ER, Nandakumar J, Cech TR. 2010. Functional interaction
533 between telomere protein TPP1 and telomerase. Genes Dev 24:613–22.
534 54. Cristofari GG, Lingner J. 2006. Telomere length homeostasis requires that
535 telomerase levels are limiting. EMBO J 25:565–574.
536 55. Xin ZT, Ly H. 2012. Characterization of interactions between naturally mutated
537 forms of the TIN2 protein and its known protein partners of the shelterin complex.
538 Clin Genet 81:301–302.
539 56. Kim SH, Beausejour C, Davalos AR, Kaminker P, Heo SJ, Campisi J. 2004. TIN2
540 mediates functions of TRF2 at human telomeres. J Biol Chem 279:43799–43804.
541 57. Bhanot M, Smith S. 2012. TIN2 stability is regulated by the E3 ligase Siah2. Mol
542 Cell Biol 32:376–384.
543 58. Yang S, Counter CM. 2013. Cell cycle regulated phosphorylation of the telomere-
544 associated protein TIN2. PLoS One 8:e71697.
545 59. Hu C, Rai R, Huang C, Broton C, Long J, Xu Y, Xue J, Lei M, Chang S, Chen Y.
546 2017. Structural and functional analyses of the mammalian TIN2-TPP1-TRF2
547 telomeric complex. Cell Res 27:1485–1502.

548 60. Chen Y, Yang Y, van Overbeek M, Donigian JR, Baciu P, de Lange T, Lei M.
549 2008. A shared docking motif in TRF1 and TRF2 used for differential recruitment
550 of telomeric proteins. Science (80-) 319:1092–1096.
551 61. Jiang J, Chan H, Cash DD, Miracco EJ, Ogorzalek Loo RR, Upton HE, Cascio D,
552 O'Brien Johnson R, Collins K, Loo JA, Zhou ZH, Feigon J. 2015. Structure of
553 Tetrahymena telomerase reveals previously unknown subunits, functions, and
554 interactions. Science (80-) 350.
555 62. Upton HE, Chan H, Feigon J, Collins K. 2017. Shared Subunits of Tetrahymena
556 Telomerase Holoenzyme and Replication Protein A Have Different Functions in
557 Different Cellular Complexes. J Biol Chem 292:217–228.
558 63. Greider CW. 2016. Regulating telomere length from the inside out: the replication
559 fork model. Genes Dev 30:1483–91.
560 64. Chen L, Redon S, Lingner J. 2012. The human CST complex is a terminator of
561 telomerase activity. Nature 488:540–544.
562 65. Feng X, Hsu SJ, Kasbek C, Chaiken M, Price CM. 2017. CTC1-mediated C-strand
563 fill-in is an essential step in telomere length maintenance. Nucleic Acids Res
564 45:4281–4293.
565 66. Zimmermann M, Kibe T, Kabir S, de Lange T. 2014. TRF1 negotiates TTAGGG
566 repeat-associated replication problems by recruiting the BLM helicase and the
567 TPP1/POT1 repressor of ATR signaling. Genes Dev 28:2477–91.
568 67. Wan M, Qin J, Songyang Z, Liu D. 2009. OB fold-containing protein 1 (OBFC1),
569 a human homolog of yeast Stn1, associates with TPP1 and is implicated in

telomere length regulation. J Biol Chem 284:26725–26731.

68. Wu P, Takai H, de Lange T. 2012. Telomeric 3' overhangs derive from resection by Exo1 and Apollo and fill-in by POT1b-associated CST. Cell 150:39–52.

69. Pinzaru AM, Hom RA, Beal A, Phillips AF, Ni E, Cardozo T, Nair N, Choi J, Wuttke DS, Sfeir A, Denchi EL. 2016. Telomere Replication Stress Induced by POT1 Inactivation Accelerates Tumorigenesis. Cell Rep 15:2170–2184.

70. Counter CM, Hahn WC, Wei W, Caddle SD, Beijersbergen RL, Lansdorp PM, Sedivy JM, Weinberg RA. 1998. Dissociation among in vitro telomerase activity, telomere maintenance, and cellular immortalization. Proc Natl Acad Sci 95:14723–8.

71. Armbruster BN, Banik SS, Guo C, Smith AC, Counter CM. 2001. N-terminal domains of the human telomerase catalytic subunit required for enzyme activity in vivo. Mol Cell Biol 21:7775–86.

72. Chiba K, Vogan JM, Wu RA, Gill MS, Zhang X, Collins K, Hockemeyer D. 2016. Endogenous TERT N-terminal tagging affects human telomerase function at telomeres in vivo. Mol Cell Biol 37:MCB.00541-16.

73. Simossis VA, Heringa J. 2003. The PRALINE online server: Optimising progressive multiple alignment on the web. Comput Biol Chem 27:511–519.

74. Simossis VA, Heringa J. 2005. PRALINE: A multiple sequence alignment toolbox that integrates homology-extended and secondary structure information. Nucleic Acids Res 33:W289–W294.

75. Pertea M, Pertea GM, Antonescu CM, Chang T-C, Mendell JT, Salzberg SL. 2015.

592 StringTie enables improved reconstruction of a transcriptome from RNA-seq
593 reads. Nat Biotechnol 33:290–295.
594 76. Kim D, Langmead B, Salzberg SL. 2015. HISAT: a fast spliced aligner with low
595 memory requirements. Nat Methods 12:357–360.
596 77. Thorvaldsdóttir H, Robinson JT, Mesirov JP. 2013. Integrative Genomics Viewer
597 (IGV): High-performance genomics data visualization and exploration. Brief
598 Bioinform 14:178–192.
599 78. Robinson JT, Thorvaldsdóttir H, Winckler W, Guttman M, Lander ES, Getz G,
600 Mesirov JP. 2011. Integrative genomics viewer. Nat Biotechnol 29:24–26.
601 79. Wang S, Pike AM, Lee SS, Strong MA, Connelly CJ, Greider CW. 2017. BRD4
602 inhibitors block telomere elongation. Nucleic Acids Res 45:8403–8410.
603 80. Morrish TA, Greider CW. 2009. Short telomeres initiate telomere recombination
604 in primary and tumor cells. PLoS Genet 5.
605

606 ## Acknowledgements

607 We would like to thank Drs. Jonathan Alder, Deborah Wuttke, Sarah Wheelan
608 and Leslie Glustrom for suggestions and help with experiments; Dr. Mary Armanios for
609 human LCL cell lines; and Dr. Andrew Holland for FLP-in cell lines. We thank Jonathan
610 Alder, Valerie Gaysinskaya, and Deborah Wuttke for critical reading of the manuscript.
611 This work was supported by NIH Grants R37AG009383 and R35CA209974 and to
612 C.W.G. and a Turock Scholar award to A.M.P.

Author Contributions

A.M.P and C.W.G designed the project and wrote the manuscript. A.M.P. performed all cloning, cell line generation, telomerase assays, and data analysis. M.A.S. performed immunofluorescence and q-FISH and passaged cell lines. J.P.O and A.M.P. performed 3'RACE and PacBio sequencing. C.J.C. prepared genomic DNA and performed Southern Blots.

Competing Interests

The authors declare they have no competing interests.

Materials and Methods

Cell Culture

Cell lines were cultured in the indicated media supplemented with 10% heat-inactivated FBS (Invitrogen, 16140071) and 1% penicillin/streptomycin/glutamine (PSG, Invitrogen 10378016). HeLa, HeLa TREx FLP-in, 293T, and 293TREx FLP-in cells were cultured in DMEM (Gibco); hTERT-RPE1 cells were cultured in DMEM/F12 (Corning); lymphoblastoid cell lines (LCLs) derived from healthy controls (samples obtained after written informed consent and approval from Johns Hopkins Medicine Institutional Review Board) were cultured in RPMI (Gibco); and K562 cell lines were cultured in IMDM (Gibco).

Expression Constructs

TIN2S cDNA was purchased from Invitrogen (Ultimate ORF IOH80607) in pENTR221. A synthetic gBlock (IDT) containing the downstream TIN2 sequence was used in Gibson Assembly to generate TIN2L. TIN2M was cloned from RT-PCR of endogenous transcripts. TIN2S, M, and L were amplified with primers containing HindIII and NotI restriction sites and an N-terminal myc tag and cloned into pcDNA5/FRT. *TINF2*, the TIN2 full-length gene inclusive of introns, was cloned into pcDNA5/FRT as described in(37). Patient mutations were generated by Site-Directed Mutagenesis. All constructs and mutants were sequence verified by Sanger sequencing at the JHU Synthesis & Sequencing Facility.

P3x-Flag-POT1-cDNA6/Myc-HisC, p3x-Flag-TPP1$_{87\text{-}544}$-cDNA6/Myc-HisC, p3x-Flag-TERT-cDNA6/Myc-HisC were a kind gift from the Cech lab(20). We introduced E169A/E171A mutations with site-directed mutagenesis to create TPP1^{TEL}. TPP1 or TPP1^{TEL}, POT1, and TERT were assembled into a single expression cassette connected by 2A peptides (Supplementary Figure 3) TERT alone was also cloned into pcDNA5. The 2A peptides leave a small tag on the downstream proteins, so TERT was cloned in the last position because it is nonfunctional with C-terminal tags(70–72). Expression cassettes are flanked by BstBI and NotI restriction sites.

Multiple Sequence Alignments

TIN2 sequences from vertebrates with known or predicted TIN2 proteins were obtained from NCBI. The longer isoform was chosen for organisms with multiple reported isoforms. Sequences were uploaded to PRALINE multiple sequence alignment using the default parameters(73, 74). To make the sequence conservation heat map, PRALINE output was imported into Microsoft Excel, and the alignment scores (0-10) of human TIN2 were colored from white=0, not conserved to navy=8-10, highly conserved. Sequences used are listed in Supplementary Table 1.

CRISPR editing

Guide RNAs were selected using the Zhang Lab CRISPR design tool (http://crispr.mit.edu/). For endogenous tagging of TIN2, the guide cgccaccaggggcgtagccaTGG was cloned into pX459-U6- Chimeric_BB-CBh-hSpCas9-2A-Puro. The repair template was generated by PCR from the cloned myc-*TINF2* construct (Supplementary Figure 1). 1μg of Cas9-2A-Puro+TIN2 guide was transfected

665 into 293T cells with 10 molar equivalents of the repair template using XtremeGENE9
666 (Roche, 6365787001). Editing was enriched with puromycin, cloned by limiting dilution,
667 and screened by PCR and restriction digest. Positive clones were examined by western
668 blot. While we found many edited clones, 293T cells are hypotriploid with an unstable
669 karyotype, and we observed high endogenous Myc expression that interfered with
670 western blotting for myc-tagged TIN2 (Supplementary Figure 1). These caveats make it
671 difficult to further study TIN2 in these knock-in cell lines.

672 **3'RACE and PacBio**
673 The 3'RACE and sequencing was performed using samples from five human cell
674 lines (293T, HeLa, RPE-1, K562, LCL) and two mouse samples (CAST/EiJ MEFs,
675 C57BL/6 liver). All mouse samples were obtained under approval by the Institutional
676 Animal Care and Use Committee at the Johns Hopkins University School of Medicine.
677 We combined 3'RACE with Pacific Biosciences (PacBio) Single-Molecule, Real-Time
678 (SMRT) sequencing to cover transcripts from the 5'UTR through the polyA tail. First, we
679 isolated mRNA $>10^6$ cells using the RNeasy Kit (Qiagen, 74104) per manufacturer
680 instructions, QIAshredder spin columns (Qiagen, 79654), on-column DNase digestion
681 (Qiagen, 79254) to remove any genomic DNA, and an RNA clean-up. Then we reverse
682 transcribed 1.5 µg mRNA with an oligo-dT_{20} primer with an adapter sequence
683 (GACTCGAGTCGACATCG-T_{20}) using the SuperScript III First Strand Synthesis Kit
684 (Qiagen, 18080-051). 5 µl of the resulting cDNA was amplified with Hot Start Phusion
685 Polymerase (Thermo, F-549L) using primers to the adapter and the 5'-UTR
686 (CGGCGACGTTTAAAGCTGA). 3-5 replicate PCR reactions were combined, purified

with the QIAquick PCR Purification Kit (QIAGEN, 28104), and submitted to the Johns Hopkins Deep Sequencing & Microarray Core Facility for sequencing. Quality control was performed on a 1:200 dilution of samples using a Bioanalyzer (Agilent, G2939A) High Sensitivity DNA Assay. Products were size selected for the expected size range of 1-3kb. 1 SMRT cell was sequenced per sample. Sequencing reads were processed in the SMRT Analysis v4.0 software, aligned to chromosome 14 with HISAT2 and assembled into potential transcripts using StringTie(75, 76). StringTie was first run for individual samples using the default settings except the minimum isoform fraction was set to 0.01 instead of 0.1. To build a gene model for all human reads, StringTie --merge was run with the minimum isoform fraction set to 0.05. HISAT2 and StringTie results were viewed in IGV(77, 78).

Western Blotting

Cells were lysed on ice in CHAPS lysis buffer (10 mM Tris-HCl, 1 mM $MgCl_2$, 1 mM EGTA, pH 8.0, 0.1 mM Benzamidine, 5 mM β-Mercaptoethanol (BME), 0.5% CHAPS, 10% Glycerol, pH 7.5) and clarified by centrifugation. Samples were denatured with 1X LDS (Invitrogen, NP0008) with 50 mM DTT and heated at 65°C for 10 minutes and separated on a 4-12% Bis-Tris gel (NuPAGE, NP0323) in 1X MOPS buffer (Invitrogen, NP0001) with 3 µl of SeeBlue Plus2 (Thermo, LC5925) prestained ladder to estimate molecular weight. Proteins were transferred to PVDF, blocked in 1X TBS + 0.1% Tween20 (TBST), 5% milk (Bio-Rad 170-6404), probed with the indicated antibodies, and developed by chemiluminesence with an ImageQuant LAS4000 imager (GE Healthcare). Primary antibodies and concentrations are as follows: mouse anti-myc

4A6 (Millipore 05-24), 1:2000; mouse anti-FLAG M2 (Sigma F1804), 1:5000; rabbit anti-tubulin (Abcam, ab6046), 1:5000. Secondary antibodies were anti-mouse IgG or anti-rabbit IgG conjugated to HRP (Cell Signaling), 1:10,000.

Co-Immunoprecipitation

Immunoprecipitations were carried out using either anti-c-myc agarose (Pierce 20168) or anti-FLAG M2 affinity gel (Sigma A2220). 20 µl of bead slurry per reaction was washed with PBS and equilibrated in CHAPS buffer before adding 45 µl lysate. Samples were incubated in an end-over-end mixer at 4°C for two hours. Beads were pelleted, washed 4 times with 300 µl 1X CHAPS buffer, and resuspended in 2X LDS loading dye for western blot analysis.

Telomerase Assays

Telomerase assay cell lines were generated in 293 TREx FLP-in cells (Invitrogen, R78007) as described(79). Briefly, parental cells were transduced with a telomerase RNA (TR) lentivirus, selected, and cloned by limiting dilution. Then, the TPP1/POT1/TERT or $TPP1^{TEL}$/POT1/TERT construct was integrated at a single site in a TR overexpressing clone using the Flp-in system (Invitrogen). For telomerase assays, 5×10^5 cells of the respective cell line were plated in each well of a 6-well dish. The next day, the indicated 2.5 µg of the indicated TIN2 or GFP construct was transfected with Lipofectamine 2000 (Invitrogen, 11668019) following the manufacturer's protocol. After 48 hours, cells were lysed in 100µl 1X CHAPS lysis buffer and clarified by centrifugation. Telomerase assays were performed as described in(79) using 5 µl of clarified cell lysate. Assays were

quantitated in ImageQuantTL (GE Healthcare) using the 15+ method as described(20). Statistical analysis was performed in GraphPad Prism.

TIN2 Overexpression Cell Lines

HeLa FLP-in cells were seeded in 6-well plates with 3 wells per construct. The next day, each well was transfected with 100 ng pcDNA5/FRT-TIN2 or -GFP construct and 900 ng pOG44 (FLP-recombinase). Wells were then pooled and selected for integration of the pcDNA5/FRT plasmid with hygromycin for 14 days. After selection, isogenic clones (> 20 per cell line) were pooled and released from selection ("week 0"). Cells were split 1:10 three times a week. No growth difference was detected. Parental HeLa FLP-in cell line was validated with STR profiling through the Johns Hopkins Genetic Resources Core Facility.

Immunofluoresence

HeLa FLP-in cells were plated in chamber slides. The following day, media was removed, the cells were washed with PBS and fixed with 4% paraformaldehyde (PFA) for 20 minutes. Slides were washed with PBS, treated with 0.5% Triton in PBS for 15 minutes, washed with PBS and blocked in 10% goat serum in PBS for 30 minutes (Sigma, G0923). Slides were incubated with a mixture of both primary antibodies for 1 hour at room temperature, washed with PBS and incubated with a mixture of both secondary antibodies for one hour at room temperature. After washing with PBS coverslips were mounted with DAPI/Vectashield. Antibodies and dilutions are as follows: mouse anti-myc clone 4A6 (Sigma, 05-724) 1:200, rabbit anti-TRF2 (Novus

Biologicals, NB110-57130) 1:800, goat anti-mouse IgG1-AlexaFluor 488 (Invitrogen, A21121) 1:400, and goat anti-rabbit IgG-AlexaFluor 555 (Invitrogen, A21429) 1:400. Slides were imaged on a Nikon Eclipse Ni-E microscope with a 60x objective using the NIS Elements software.

Telomere Southern Blots

Genomic DNA was prepared from ~3-6 x 10^6 frozen cell pellets lysed in Nuclei Lysis Solution (Promega, A7941), treated with RNAse A (10mg/ml, Roche) and overnight with Proteinase K (400mg/ml, ThermoFisher), followed by salting out of the proteins with Protein Precipitation Solution (Promega, A7951). The genomic DNA was precipitated with isopropanol and resuspended in TE (10mM Tris pH8.0, 1mM EDTA). Approximately 2µg of genomic DNA, quantitated by a Qubit 3.0 Fluorometer (Life Technologies), was cut with the restriction enzyme with MseI (NEB, R0525M) overnight, run on a Southern blot, and hybridized with a radiolabeled telomere fragment from JHU821 as described(79). Images were captured, converted, and quantitated from Storage Phosphor Screens (GE Healthcare) as described in(79).

Telomere analysis by q-FISH

For metaphase Fluorescent in situ hybridization (FISH) analysis, cultures were first arrested in with Karyomax Colcemid (Invitrogen) for 6-7 h. The cells were trypsinized in 0.05% Trypsin-EDTA (Gibco), washed in PBS, swelled with 0.075M KCl at 37°C for 15 min and fixed in methanol:acetic acid (3:1). Cell suspensions were then dropped onto chilled slides and dried overnight. FISH was performed using a Cy3-labeled $(CCCTAA)_3$ PNA oligonucleotide (PE Biosystems). Metaphase spreads were

774 counterstained with DAPI/Vectashield. Slides were blinded during image acquisition and
775 analysis. Images were acquired using a Nikon Eclipse NI-E microscope and NIS
776 Elements software. Telomere fusions, fragile telomeres, and signal-free ends were tallied
777 in 10-metaphases per sample in a total of three replicates. Telomere length was measured
778 in TFL-Telo V2.0, and outliers were analyzed as described(80) to determine PQ ratios
779 and sister-telomere ratios. Histograms of telomere lengths were generated in GraphPad
780 Prism.

781 # Figures

782

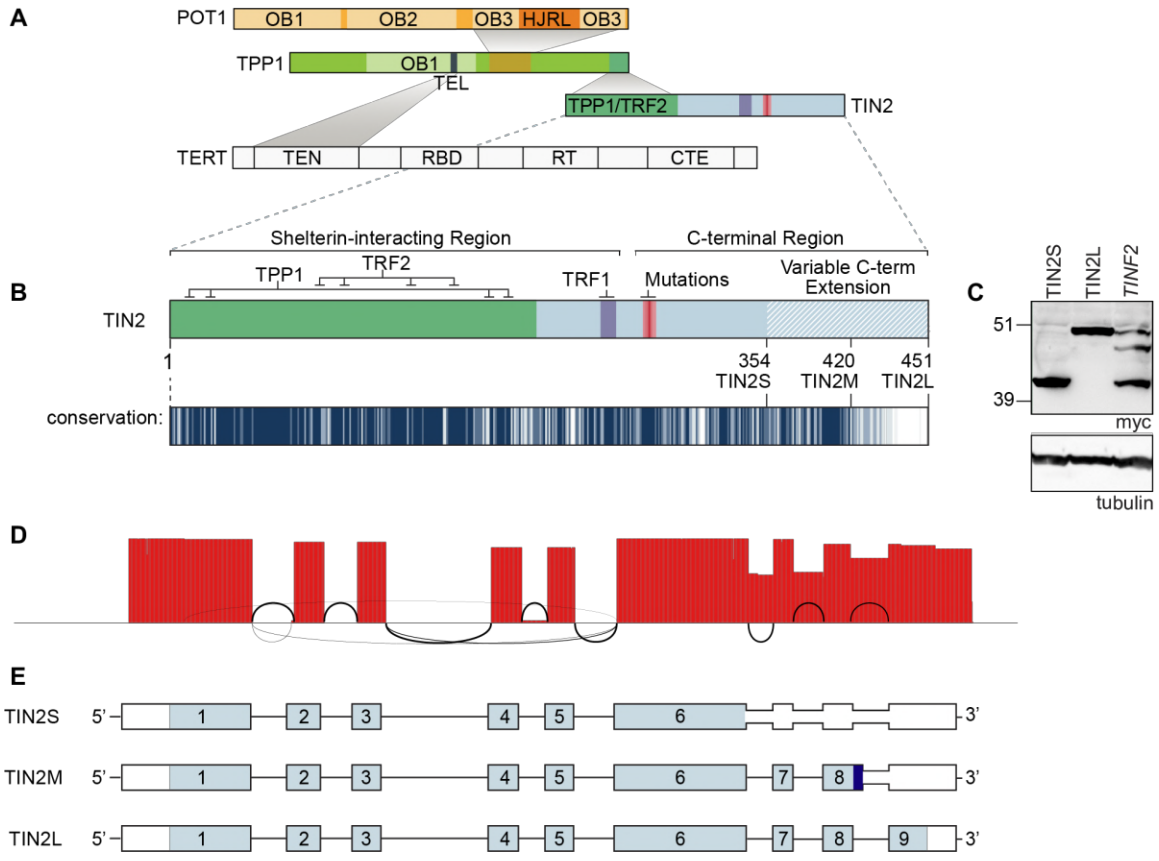

Figure 1. TIN2 has three predominant isoforms in human cells.
a, Schematic of TIN2, TPP1, and POT1 interaction. The TIN2 N-terminal domain interacts with the C-terminus of TPP1, which is part of a telomerase processivity complex. TPP1 heterodimerizes with the POT1 OB3 domain and also directly interacts with the TERT TEN-domain through a TEL-patch motif. **b**, Detailed schematic of the TIN2 protein. TRF2/TPP1 interaction domain is indicated in green with simplified TPP1 and TRF2 contacts illustrated above. TRF1 FxLxP interaction motif is indicated in purple. The red gradient indicates the patient mutation cluster, where mutated residues cluster but vary in their frequency and disease severity. Light blue hatched region indicates the variable C-terminal extension. Below is a conservation track generated from the values from a multiple sequence alignment with 35 known or predicted TIN2 proteins (see Methods and Supplementary Table 1); colored white = 0, not conserved to navy = 10, highly conserved. **c**, Myc western blot of overexpressed cDNA for TIN2S and TIN2L and the full-length myc-*TINF2* gene. **d**, Sashimi plot of the 3'RACE PacBio sequencing reads aligned to *TINF2*. Height indicates coverage and black lines indicate splicing events, where the line weight corresponds to the frequency of usage. **e**, StringTie-generated TIN2 transcripts from combined data from 293T, HeLa, RPE-1, K562, and LCL cell lines showing TIN2S, TIN2L, and the new isoform, TIN2M. light blue = coding sequence; darker blue = unique TIN2M sequence; white = untranslated region.

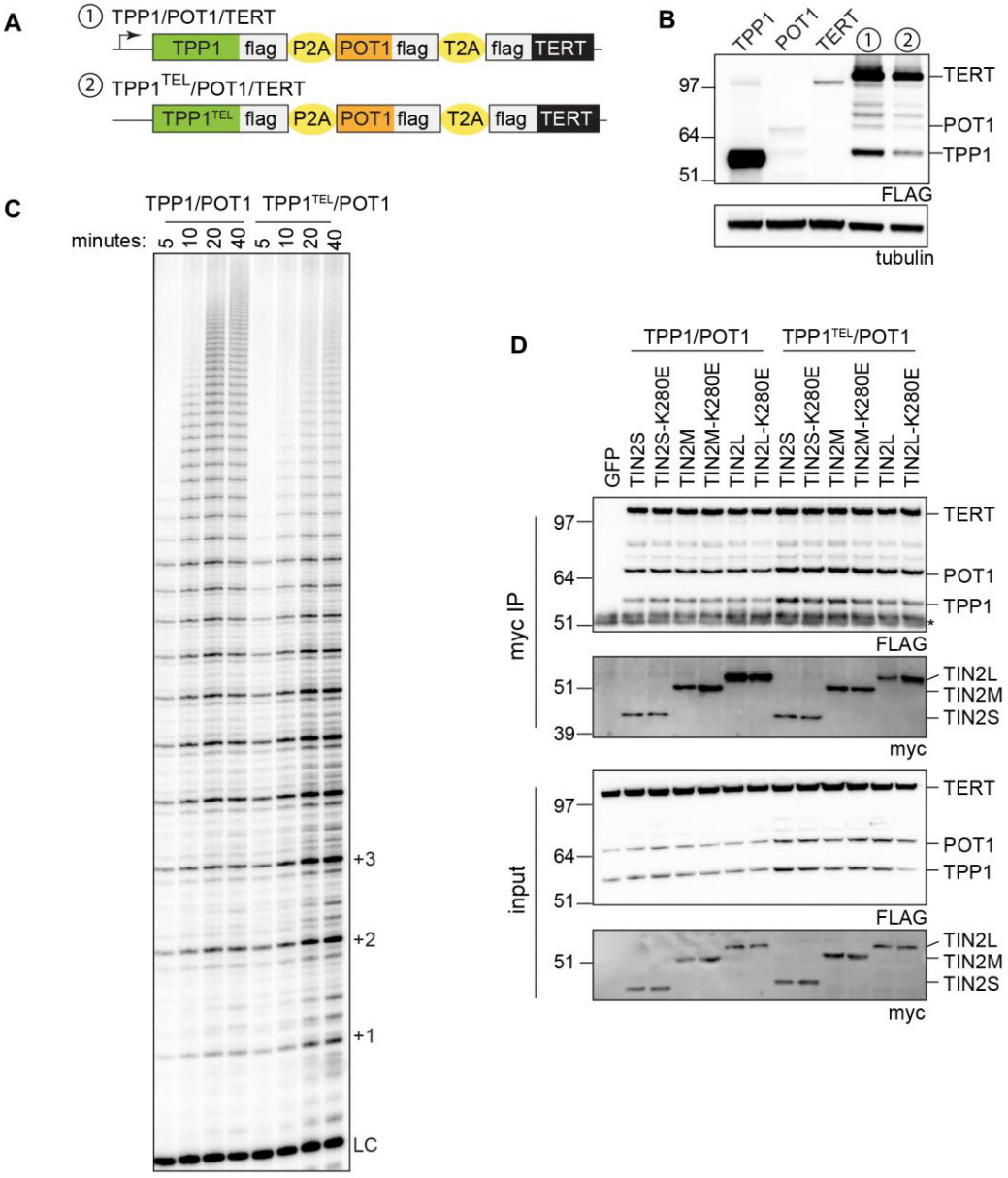

Figure 2. TIN2 isoforms form a complex with TPP1/POT1 that binds telomerase and is not disrupted by the K280E mutation.

a, Expression cassettes used in this study. All cassettes are expressed by the CMV promoter in the pcDNA5/FRT backbone. Telomerase assay cell lines were generated as described in the Methods. **b**, Western blot of individually transfected TPP1, POT1, and TERT cDNAs next to telomerase assay cell lines numbered as in **a**. FLAG bands above POT1 are unidentified but may be TERT degradation products. **c**, Telomerase assays stopped at 5, 10, 20, and 40 minutes for each cell line. Telomere repeats are indicated by

+1, +2, etc. LC = loading and purification control. **d**, Co-immunoprecipitation of TERT, TPP1, and POT1 with TIN2 using anti-myc agarose beads in both telomerase assay cell lines 1 and 2 transfected with TIN2S, TIN2M, or TIN2L. Similar co-IP levels were observed in both WT and mutant constructs. *, IgG bands.

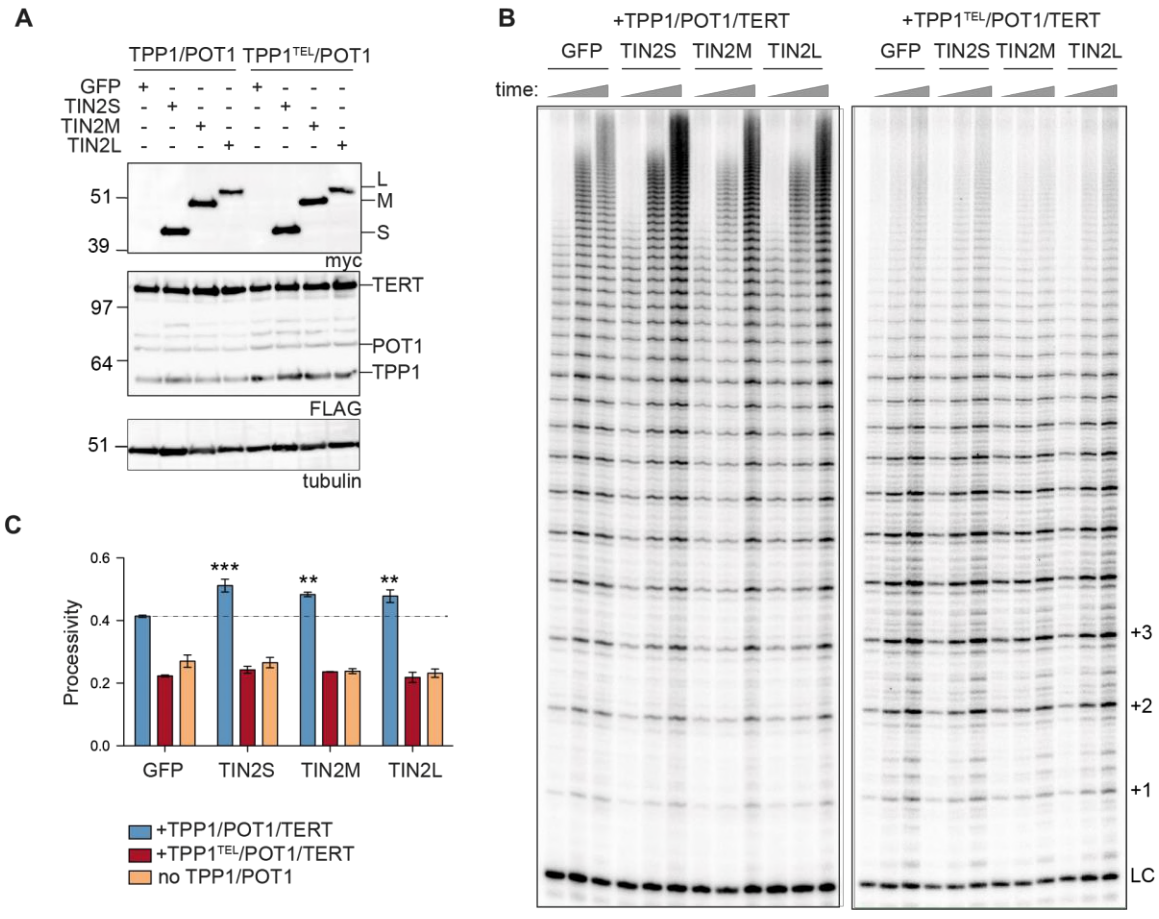

Figure 3. TIN2 stimulates telomerase processivity beyond the TPP1/POT1 stimulation

a, Western blots of GFP and myc-TIN2 isoform transfections into TPP1/POT1/TERT (left) or TPP1^{TEL}/POT1/TERT (right) cell lines. FLAG bands above POT1 are unidentified but may be TERT degradation products. **b**, Telomerase assays stopped at 10, 20, and 40 minutes. Quantification is shown in (C). Increasing time indicated by the grey triangle. LC, loading and purification control; +1, +2, +3 indicates repeat number. **c**, Mean processivity values from 3 independent telomerase assays at the 40 minute timepoint using the 15+ processivity method (see Methods). Orange bars are from a cell line overexpressing TERT/TR but not TPP1/POT1 (Supplementary Figure 6). Data was analyzed with a one-way ANOVA and Bonferroni's Multiple Comparisons test against the GFP control. n=3 independent transfections per cell line indicated. Error bars represent SD. **, $p<0.01$; ***, $p<0.001$.

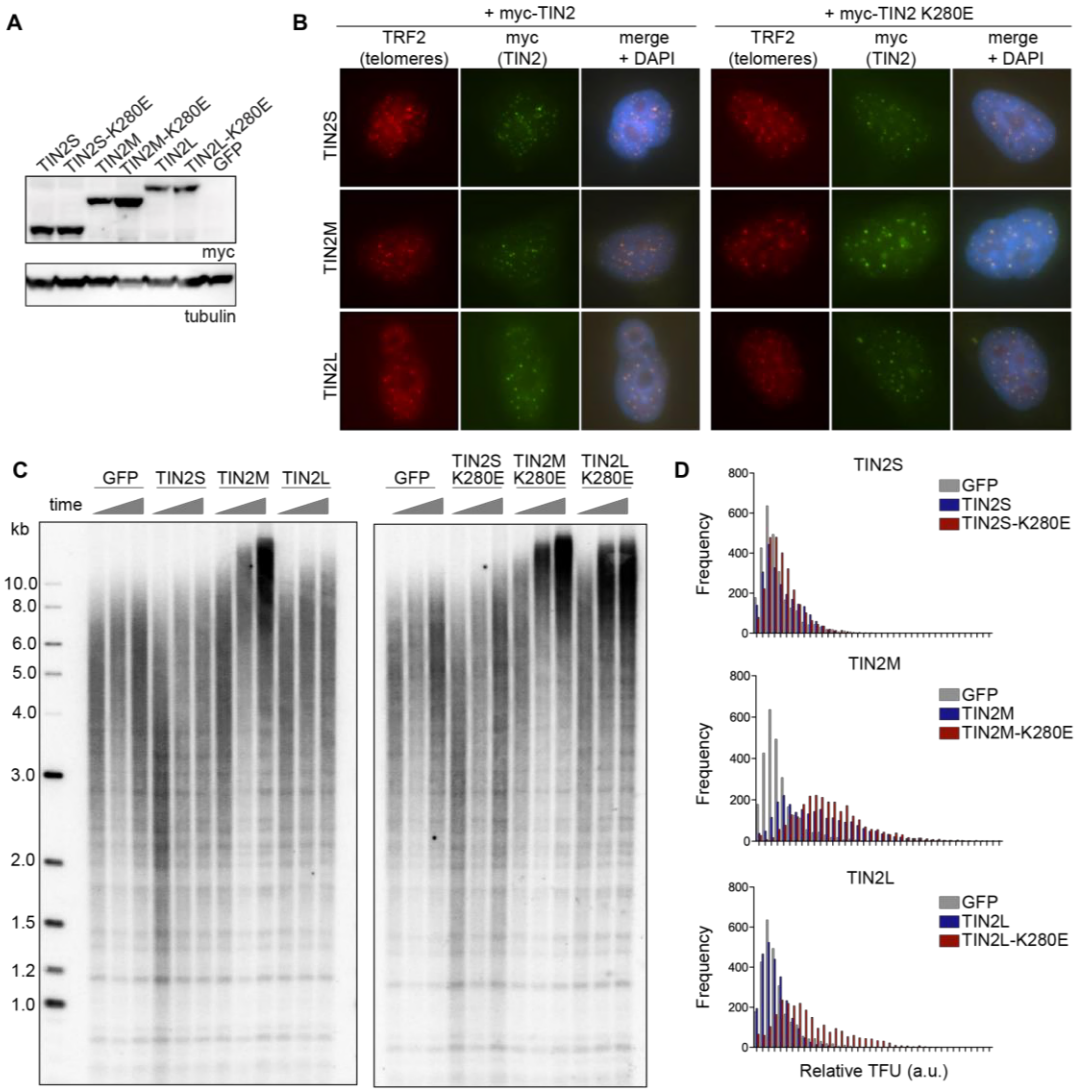

831

832 **Figure 4. TIN2 isoforms localize to telomeres but have different effects on telomere**
833 **length.**
834 **a**, Western blot of myc-TIN2 overexpressing HeLa FLP-in cell lines. **b**,
835 Immunofluorescence of TIN2 expressing cell lines. TRF2 marks telomeres (red), anti-
836 myc antibody marks TIN2 (green), and nuclei were counterstained with DAPI. Merge
837 image shows telomeric foci with colocalized TRF2 and TIN2 staining. **c**, Telomere
838 Southern blot of genomic DNA from HeLa-TIN2 cell lines. Three timepoints indicated
839 by grey triangles refer cells harvested at 3, 8, and 13 weeks in culture. Left, 2-log ladder
840 values in kb. **d**, Histograms of telomere intensities from quantitative telomere FISH (q-
841 FISH) on late passage metaphase chromosomes in the indicated cell lines, separated by

842 isoform. The same GFP sample is plotted on each graph. Relative telomere fluorescence
843 units (TFU) on the x-axis reflects telomere length. In each, grey = GFP, blue = TIN2-
844 WT, red = TIN2-K280E.

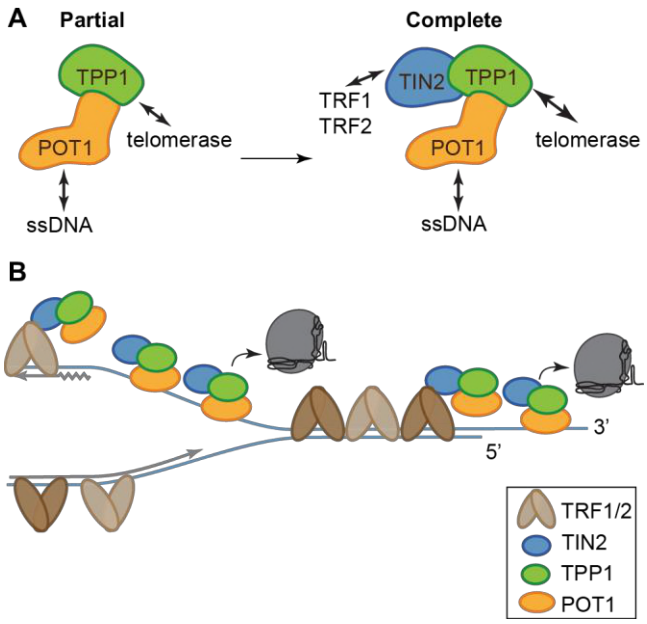

Figure 5. TIN2/TPP1/POT1 is a stable shelterin subcomplex.
a, TIN2 completes the telomerase processivity complex. TIN2 enhances TPP1/POT1 stimulation of telomerase, forming a heterotrimeric processivity complex that is recruited to the telomere through TRF1/2 interactions. **b**, A dynamic, heterogeneous distribution of shelterin proteins across the length of human telomeres coordinates telomere length maintenance. TRF1 and TRF2 may direct TIN2/TPP1/POT1 to single-stranded DNA both at the telomere overhang and within the replication fork, aiding its roles in fork progression and telomerase stimulation.